Density functional and quasiparticle band-structure calculations for $Ga_xAl_{1-x}N$ and $Ga_xIn_{1-x}N$ alloys

F. Sökeland, M. Rohlfing, P. Krüger, and J. Pollmann
Institut für Festkörpertheorie, Universität Münster, Wilhelm-Klemm-Strasse 10, 48149 Münster, Germany
(Received 21 February 2003; revised manuscript received 27 May 2003; published 8 August 2003)

We investigate the electronic structure of two wide-band-gap semiconductor alloys $Ga_xAl_{1-x}N$ and $Ga_xIn_{1-x}N$, employing three different *ab initio* band-structure approaches. Local density calculations within density functional theory using conventional as well as self-interaction-corrected pseudopotentials and quasiparticle band-structure calculations are carried out. The stochastical alloy problem is treated within the virtual crystal approximation, as well as within a cluster expansion approximation. One main issue is the evaluation of the bowing of the composition dependence of the fundamental band gap. It turns out that the band-gap bowing for $Ga_xAl_{1-x}N$ alloys is described reasonably well within the virtual crystal approximation. For $Ga_xIn_{1-x}N$, on the contrary, that approximation does not correctly describe the composition dependence of the band gap because it neglects significant local structural relaxations. These are taken into account in the cluster expansion approximation. Our results indicate that in both alloys the band gap exhibits a composition-dependent bowing function rather than a constant bowing parameter.

DOI: 10.1103/PhysRevB.68.075203 PACS number(s): 71.20.Nr, 71.23.−k, 71.22.+i

I. INTRODUCTION

The electronic structure of alloys has gained renewed interest during recent years because of the growing technological importance of wide-band-gap semiconductors. Alloying of such semiconductors is of significant importance for the development of optoelectronic devices and detectors. The possibility to tune the wavelength of emitted light through a wide spectral region makes it feasible to design novel compound semiconductors. Suitable candidates for wide-band-gap alloys can be found among the III-V and II-VI materials. Especially the III nitrides AlN, GaN, and InN are of importance in the field of optoelectronics and a huge amount of experimental and theoretical work has focused on their electronic and structural properties.[1] Ternary alloys like $Ga_xAl_{1-x}N$ and $Ga_xIn_{1-x}N$ can be fabricated whose fundamental electronic transitions can be tailored from the ultraviolet (AlN) across the visible violet/blue (GaN) to the visible yellow (InN) regions of the spectrum.

The theoretical description of semiconductor alloys faces two main problems. (i) The lack of translational symmetry hinders the use of conventional solid-state techniques designed for periodic systems. (ii) In addition, the electronic and optical spectrum of semiconductors is strongly affected by many-body correlation effects among the electrons. A number of approaches have been developed to address non periodic alloys. We focus on two such techniques: i.e., the *virtual crystal approximation* (VCA) (Refs. 2 and 3) and the *cluster expansion approximation* (CEA) (Ref. 4–6). The many-body correlation effects can be treated to different levels of complexity and accuracy. We employ not only the local density approximation (LDA) of density functional theory (DFT) but also self-interaction-corrected DFT,[7,8] as well as many-body perturbation theory in the *GW* approximation (GWA).[9,10]

The VCA is a computationally very efficient approach to the electronic structure of alloys. In this approximation, the random alloy is simulated by a periodic crystal of ''virtual atoms'' that represent a weighted average of the alloy components. Due to the enforced periodicity, the VCA can be implemented in any standard electronic structure method with the numerical demand being no larger than that for a periodic lattice. Due to its moderate computational effort, the VCA is a very useful approach for a first attempt to investigate a number of fundamental questions concerning the electronic structure of wide-band-gap semiconductor alloys. In particular, we use the VCA to scrutinize the influence of quasiparticle corrections on the alloy band structure. In some cases, simple alloy theories like the VCA do not apply and more involved methods like a cluster expansion approximation need to be employed. The CEA belongs to the class of so-called lattice theories. They consist of expanding a physical quantity into a set of contributions from elementary clusters. Since the clusters are periodically repeated,[11] standard solid-state techniques can be applied to the resulting supercells to obtain the relevant quantities of the clusters which are then statistically averaged. A detailed discussion of the formalism can be found in Ref. 12, and some of its practical aspects are compiled in the following sections. The cluster expansion approximation has been applied also, e.g., by Bechstedt and co-workers[13,14] in their detailed studies of the structural, electronic, and thermodynamic properties of strained group-III nitride alloys.

In the present work we report on VCA and CEA calculations for $Ga_xAl_{1-x}N$ and $Ga_xIn_{1-x}N$ alloys in the zinc-blende structure. We are especially interested in the fundamental electronic transition energies and their nonlinear dependence on the concentration x: i.e., in their bowing behavior. The dependence of a physical quantity Ω of a ternary alloy $A_xB_{1-x}C$ on x can often be described accurately by a parabola

$$\Omega(x)=x\Omega_{AC}+(1-x)\Omega_{BC}+bx(1-x), \qquad (1)$$

with a *bowing parameter b* which describes the overall deviation from the linear interpolation between Ω_{AC} and Ω_{BC}. Whenever a constant bowing parameter b without further specification is mentioned in this work, it refers to such a quadratic fit. The situation becomes more complicated if Ω depends in a nonquadratic manner on x. In this case a *concentration-dependent* bowing function $b(x)$ can be defined as

$$b(x)=\frac{\Omega(x)-x\Omega_{AC}-(1-x)\Omega_{BC}}{x(1-x)}. \tag{2}$$

If defined in this way, $b(x)$ constitutes (at each x) a relationship between $\Omega(x)$ and the end-point values Ω_{AC} and Ω_{BC}. Note that $b(x)$ as defined in Eq. (2) does not coincide with the second derivative $-1/2\ \partial^2\Omega/\partial x^2$ (which would be another possibility of defining a concentration-dependent bowing). Also, note that the average parameter b as defined in Eq. (1) does not necessarily equal the concentration average of $b(x)$. In many cases, the concentration-dependent $b(x)$ approximately shows a linear dependence on x.

Before focusing on the alloys, we give a short summary of the electronic structure of their bulk constituents AlN, GaN, and InN.[1] These nitrides occur both in the hexagonal wurtzite and the cubic zinc-blende structure, the latter of which is in the focus of our work.

The existence of cubic AlN has been reported by Schwabe and Mader[15] and by Gerthsen and co-workers.[16] *Ab initio* calculations predict cubic AlN to be an indirect semiconductor (minimum transition $\Gamma_{15}^{v}\rightarrow X_1^c$) with a LDA band gap of $E_g^{LDA}=3.2$ eV and a quasiparticle (QP) band gap of $E_g^{QP}=4.9$ eV.[17] To our knowledge there is no experimental verification of these results, up to now.

Cubic GaN, on the other hand, is a direct semiconductor. Optical absorption measurements[18–20] yield a band gap of $E_g^{GaN}=3.2$ eV which compares reasonably well with the quasiparticle band gaps of $E_g^{QP}=3.1$ eV and $E_g^{QP}=3.6$ eV, as obtained by Rubio *et al.*[17] and by some of the present authors,[10] respectively. DFT-LDA calculations, on the other hand, yield a band gap of $E_g^{LDA}=2.0$ eV showing the typical underestimation of the fundamental gap in LDA. If the Ga $3d$ states are explicitly included within the pseudopotentials as valence states, the LDA band gap even reduces to $E_g^{LDA}=1.1$ eV. The Ga $3d$ states are found at -13.6 eV, being in resonance with the N $2s$ state. DFT calculations using self-interaction and relaxation-corrected pseudopotentials[7] (DFT-SIRC) are able to lift this *sd* degeneracy and correctly predict the energetic position of the $3d$ states at -16.7 eV which is now below the N $2s$ band. In addition, the band gap increases to $E_g^{SIRC}=3.5$ eV and matches the experimental value much more closely than the LDA result.

The low thermal stability of cubic InN makes this compound semiconductor the least-studied group-III nitride. It has been observed that InN is a direct semiconductor with a band gap of $E_g^{InN}=1.9$ eV.[21] When using a conventional In($5s$,$5p$) pseudopotential we find a very small LDA band gap of $E_g^{LDA}=0.2$ eV (in agreement with the results of Ref.22). If the chemically active indium $4d$ semicore electrons are included among the valence electrons by using an In($4d$,$5s$,$5p$) pseudopotential, we obtain a semimetallic inverted band structure with a negative LDA band gap of $E_g^{LDA}=-1.0$ eV. All-electron LDA linear muffin-tin orbital (LMTO) calculations also report an inverted band structure with E_g between -0.1 eV (Ref. 1) and -0.4 eV (Ref. 23). It has been shown that this inversion, which is an artifact of the LDA, can be overcome by including self-interaction corrections.[7,8] In DFT-SIRC the band gap results as $E_g^{SIRC}=1.3$ eV in much closer agreement with experiment.

II. METHODS

Many of our calculations employ density functional theory together with the local density approximation to solve the electronic structure problem. In some cases we also include self-interaction and relaxation corrections[7] to compensate the artificial self-interaction of electronic states within the LDA. Such SIRC-DFT calculations have been shown[7] to yield band gaps of heteropolar wide-band-gap semiconductors (GaN, ZnO, etc.) in very good agreement with measured data. In addition, we also carry out quasiparticle calculations in order to scrutinize whether the LDA gap problem has an important influence on band-gap bowing. The QP corrections of the LDA band structure are evaluated within the *GW* approximation of the electron self-energy operator.[9,10] The GWA yields highly accurate band structures for a large variety of systems and thus constitutes the state of the art for calculating electronic spectra. It should, therefore, serve as a reliable basis for the determination of band-gap bowing, as well.

The wave functions are expanded in a basis of atom-centered Gaussian orbitals of *s*, *p*, *d*, and *s** symmetry with several decay constants per atom.[24] These basis sets are found to be sufficiently flexible to guarantee basis-set convergence at all concentrations x. All elements (Al,Ga,In,N) are described by norm-conserving *ab initio* pseudopotentials (PP's) of the Hamann type,[25,26] except for the SIRC calculations that require specific pseudopotentials.[7]

If not stated otherwise, we employ pseudopotentials that treat the conventional valence orbitals as valence states (i.e., Al $3s^2p^1$, Ga $4s^2p^1$, In $5s^2p^1$, and N $2s^2p^3$). For Ga and In, we label these potentials "3+ pseudopotentials" referring to the three valence electrons. The *d* states of the Ga and In semicore shells (i.e., Ga $3d$ and In $4d$, respectively) have a significant influence on the structural and electronic properties of $Ga_xIn_{1-x}N$. This can be taken into account in a straightforward way by including the *d* states among the valence states in the pseudopotential construction, leading to potentials that we label "13+ pseudopotentials," referring to the 13 valence electrons (Ga $3d^{10}4s^2p^1$ and In $4d^{10}5s^2p^1$, respectively) described by them.

A. Virtual crystal approximation

The majority of VCA calculations have been carried out within empirical[27] and semiempirical[28] electronic structure techniques. Recently various procedures to implement the

VCA within *ab initio* techniques, employing norm-conserving pseudopotentials, have also been suggested.[29] The method we present here relies on the mixing of ionic *ab initio* pseudopotentials that are transferred to the solid to model the VCA alloy. In the first step we construct norm-conserving pseudopotentials for Al, Ga, In, and N according to Hamann's recipes.[25] For each concentration x and each angular momentum l the pseudopotentials for the cationic sublattice (e.g., for $Ga_xAl_{1-x}N$) are linearly averaged on a radial grid:

$$V_{l,ion}^{PS}(r,x) = xV_{l,ion}^{\mathrm{Ga}}(r) + (1-x)V_{l,ion}^{\mathrm{Al}}(r). \tag{3}$$

All effective potentials are tested for the free Ga_xAl_{1-x} and Ga_xIn_{1-x} ''virtual atoms'' to see how the atomic energy levels evolve as a function of concentration and to obtain the radial atomic wave functions $R_l^{PS}(r,x)$. The latter are finally used to transform the semilocal effective pseudopotential to its separable form.[30]

B. Cluster expansion approximation

For alloys that show significant structural relaxations induced by lattice mismatch simple *mean-field* theories, like the VCA, often suffer from lack of accuracy. One example is $Ga_xIn_{1-x}N$ due to the 10% lattice mismatch between GaN and InN. In such materials more involved methods must be invoked. Such a method is the CEA which belongs to the class of lattice theories and mainly consists in expanding a physical quantity into a set of contributions of elementary clusters. Periodic repetition of these clusters, as suggested by Conolly and Williams,[11] leads to representative periodic systems to which Bloch's theorem can be applied. Within the Conolly-Williams approach the alloy concentration x is directly linked to its respective lattice constant $a(x)$. For a detailed discussion we refer the reader to the literature.[12] In our present approach we restrict ourselves to the so-called tetrahedron approximation and use simple cubic unit cells containing eight atoms—i.e., four nitrogen atoms at the anion sites and either Ga or In atoms at the four cation sites. There are five different cation site configurations of such clusters: In_4N_4, In_3GaN_4, $In_2Ga_2N_4$, $InGa_3N_4$, and Ga_4N_4. Within the cubic eight-atom unit cell there is only one inequivalent configuration for each of these five clusters. In a totally random alloy, the configuration $Ga_nIn_{(4-n)}N_4$ occurs with a binomial probability of $\binom{4}{n}x^n(1-x)^{4-n}$. Within this tetrahedron approximation, the statistical average of, e.g., the band gap E_g is thus finally given by

$$E_g(x) = \sum_{n=0}^{4} \binom{4}{n} x^n(1-x)^{4-n} E_g^{[n]}(a(x)), \tag{4}$$

with $E_g^{[n]}(a)$ being the gap of the $Ga_nIn_{(4-n)}N_4$ structure with lattice constant a. If not stated otherwise, $a(x)$ is the linear interpolation between the lattice constants of the two constituents according to Vegard's law[31] and the electronic structure of each configuration (i.e., for each n) is obtained by using ideal crystal geometries.

The CEA can also be used to *calculate* the composition-dependent lattice constant, thus going beyond Vegard's assumption[31] of a being linear in x. To do this we calculate the total energies as a function of the concentration x *and* the lattice constant a as independent variables,

$$E_{tot}(x,a) := \sum_{n=0}^{4} \binom{4}{n} x^n(1-x)^{4-n} E_{tot}^{[n]}(a), \tag{5}$$

and then minimize these energies with respect to a:

$$\min_a E_{tot}(x,a) \Rightarrow a(x). \tag{6}$$

Another issue related to the structure concerns the internal relaxations of each configuration. Since the cations differ in size, there will be internal relaxations within the $Ga_nIn_{4-n}N_4$ clusters due to bond length contractions and expansions which break the tetrahedral symmetry.

From the optimized internal structure of each cluster one can calculate the concentration dependence of bond lengths, e.g., of $d_{\mathrm{Ga\text{-}N}}(x)$ by using

$$d_{\mathrm{Ga\text{-}N}}(x) = \sum_{n=0}^{4} \binom{4}{n} x^n(1-x)^{4-n} d_{\mathrm{Ga\text{-}N}}^{[n]}. \tag{7}$$

The CEA thus allows us to investigate the influence of both volume relaxations (lattice constant) and binding relaxations (bond lengths and angles) on the band-gap bowing.

Note that the tetrahedron approximation is only useful for physical quantities that are dominated by short-range properties like the interatomic chemical bonds and quantities associated with them. Properties of long-range nature may require much larger clusters to be accurately described by the CEA.

III. RESULTS FOR $Ga_xAl_{1-x}N$

Before we present the results from our LDA and GWA calculations in Secs. III B and III C, we first briefly summarize a number of results from the literature.

A. Data from the literature

The cubic III-V alloy $Ga_xAl_{1-x}N$ has attracted much interest due to its prospects in fabricating optical devices emitting from the blue to the near ultraviolet. The system was first synthesized by an epitaxial growth process on sapphire.[32] The lattice constant of $Ga_xAl_{1-x}N$ has experimentally been shown[33] to follow Vegard's law. Later on, some investigations focused on determining the band-gap bowing parameter. Since GaN is a direct semiconductor while AlN is indirect, a direct-indirect transition occurs at a concentration x_t. Recent calculations yield x_t in the range from 0.41 to 0.48 (see Table I).

There have been several theoretical and experimental investigations of $Ga_xAl_{1-x}N$ (see Table I). Empirical VCA calculations by Fan *et al.*[27] and semiempirical VCA investigations by Pugh *et al.*,[28] as well as LMTO cluster expansions by Albanesi *et al.*[34] and Agrawal *et al.*,[35] have been reported. In all these calculations a nearly linear concentration dependence of the band gap ($b \approx 0.0$ eV) has been found. A plane-wave[36] and a linear combination of atomic

TABLE I. Theoretical and experimental results from optical spectroscopy for the average band-gap bowing b in zinc-blende $Ga_xAl_{1-x}N$ alloys from the literature. The column "Transition" shows the concentrations x_t for which an indirect-to-direct transition of the band gap takes place.

Method	b [eV]	Transition
VCA[a]	-0.05	0.48
VCA[b]	≈ 0.00	0.43
LMTO CEA[c]	≈ 0.00	0.43
LMTO CEA[d]	≈ 0.00	0.41
PW-PP[e]	-0.53	–
LCAO-PP[f]	-0.56	–
Experiment[g]	-0.80	–
Experiment[h]	-1.00	–
Experiment[i]	-1.00	–
Experiment[j]	-0.98	–
Experiment[k]	≈ 0.00	–
Experiment[l]	≈ 0.00	–

[a]Reference 27.
[b]Reference 28.
[c]Reference 34.
[d]Reference 35.
[e]Reference 36.
[f]Reference 37.
[g]Reference 38.
[h]Reference 39.
[i]Reference 40.
[j]Reference 41.
[k]Reference 42.
[l]Reference 43.

orbitals (LCAO)[37] pseudopotential calculation have yielded considerably stronger bowing of -0.53 eV and -0.56 eV, respectively.

In an experiment, Yoshida *et al.*[38] have determined a bowing of -0.8 eV. Koide *et al.*[39] observed a band-gap bowing of $b=-1.0$ eV by measuring the optical absorption spectrum of $Ga_xAl_{1-x}N$ films prepared by metalorganic chemical vapor deposition (MOCVD) for x between 0.6 and 1.0. Itoh *et al.*[40] extended the growth method by using AlN buffer layers to obtain higher-quality crystalline films. They also found $b=-1.0$ eV for the bowing parameter. Finally, photoluminescence spectra recorded by Khan *et al.*[41] for $0.76 \leqslant x \leqslant 1.0$ resolved a bowing parameter of $b=-0.98$ eV. On the other hand, Khan *et al.*,[42] as well as Wickenden *et al.*,[43] measured $b \approx 0.0$ eV although these authors used basically the same growth techniques. The origin of these experimentally determined deviations in the bowing parameter ($b=-1.0$ eV$\leftrightarrow b \approx 0.0$ eV) is still unclear. Further below we try to rationalize these discrepancies between the various experiments by discussing the role of restricted concentration intervals used in some of the works cited above.

B. VCA calculations within the DFT-LDA

We start our investigations by mixing the unscreened ionic 3+ pseudopotentials of Al and Ga for various concentrations on a radial grid. The resulting potentials—representing mixed Ga_xAl_{1-x} "virtual atoms"—are tested with respect to their atomic levels. The LDA energies of the valence s level (with Al $3s$ and Ga $4s$ at the end points) and the valence p level (with Al $3p$ and Ga $4p$ at the end points) depend on x in a slightly nonlinear way with a small bowing parameter of $b_s=+0.25$ eV for the s level and $b_p=-0.01$ eV for the p level. In the next step we transfer the effective potentials to the solid. The lattice mismatch between AlN and GaN amounts to some 3%, only. Therefore, we assume in agreement with Ref. 33 that the lattice constant of $Ga_xAl_{1-x}N$ follows Vegard's law:

$$a(x)=\{4.50x+4.37(1-x)\} \ \text{Å}. \tag{8}$$

We calculate the band structure for each concentration x from 0.0 to 1.0 in steps of 0.2. Figure 1 shows the resulting direct ($\Gamma_{15}^v \rightarrow \Gamma_1^c$) and indirect ($\Gamma_{15}^v \rightarrow X_1^c$) band gaps by solid and open circles. The lines for all x values interpolating between the calculated values are determined by a quadratic fit according to Eq. (2). Both band gaps are characterized by a weakly nonlinear concentration dependence with a small downward bowing of $b_{dir}^{LDA}=-0.15$ eV for the direct band gap and $b_{ind}^{LDA}=-0.10$ eV for the indirect $\Gamma_{15}^v \rightarrow X_1^c$ transition. This seems to be in reasonable agreement with the previous experimental and theoretical results of $b \approx 0$. In addition—and in agreement with other calculations (see Table I)—we predict the *indirect-to-direct* transition to occur at $x_t^{LDA}=0.46$ (see Table II). At the transition concentration the band gap of the $Ga_xAl_{1-x}N$ alloy amounts to $E_g^{LDA}(x_t^{LDA})=2.9$ eV.

A more detailed analysis of the data shown in Fig. 1 reveals that the dependence of the band gaps on concentration is not strictly quadratic, indeed. For a better comparison with other theoretical and experimental work, we fit our $b(x)$ results by a linear function of x. For the direct band gap we then find a concentration-dependent bowing function $b(x)$

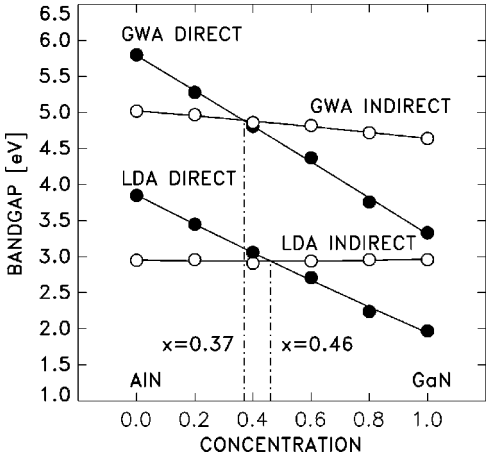

FIG. 1. Concentration-dependent band gap of $Ga_xAl_{1-x}N$, calculated within the VCA employing the DFT-LDA (lower curves) and the GWA (upper curves), respectively. Both the direct ($\Gamma_{15}^v \rightarrow \Gamma_1^c$) transition (solid circles) and the indirect ($\Gamma_{15}^v \rightarrow X_1^c$) transition (open circles) are displayed. The intersection points between direct and indirect band gaps mark the LDA ($x_t^{LDA}=0.46$) and GW ($x_t^{QP}=0.37$) transition concentrations. It should be noted that in this and the following figures the symbols show results as calculated for the particular x values in steps of 0.2. The connecting lines result from a quadratic fit of the points according to Eq. (2).

TABLE II. VCA bowing parameters and their concentration dependences for the direct band gap of zinc-blende $Ga_xAl_{1-x}N$ as calculated in this work. The column "Transition" shows the concentrations x_t for which an indirect-to-direct transition of the band gap takes place.

Method	$b(x)$ [eV]	$b(0.9)$ [eV]	b [eV]	Transition
DFT-VCA	$-0.71x+0.10$	-0.54	-0.15	0.46
QP-VCA	$-0.25x+0.04$	-0.19	$+0.05$	0.37

$\approx(-0.71x+0.1)$ eV (see Table II). This may provide an explanation for the difference between the experimentally observed bowing parameters. The average bowing parameter of $b_{dir}^{LDA}=-0.15$ eV, obtained from a quadratic fit to $E_{gap}(x)$ and considered valid for the entire concentration range, is indeed very weak. This corresponds to the experimental data discussed by Khan *et al.*[42] and Wickenden *et al.*[43] The experiments by Koide *et al.*,[39] Itoh *et al.*,[40] and Khan *et al.*,[41] on the other hand, that have been carried out at much higher concentrations between $x=0.7$ and $x=1.0$, exhibit a quite significant bowing of $b\approx-1$ eV. For such high concentrations, our bowing function $b(x)$, indeed, yields a significant bowing of, e.g., $b(0.9)=-0.54$ eV.

We summarize our DFT-VCA results in three statements: (i) The virtual crystal approximation within the LDA is a useful approximation to calculate the electronic structure of $Ga_xAl_{1-x}N$ alloys. (ii) The VCA formulation in terms of *ab initio* pseudopotentials is a practicable extension of empirical VCA implementations. (iii) The band gaps of the alloys are characterized by a concentration-dependent bowing function $b(x)$. The direct LDA band gap, e.g., reaches a substantial bowing of $b(x)=-0.61$ eV at $x=1.0$. The average bowing of the band gap, on the other hand, which is obtained from a quadratic fit at all x values, is rather weak.

C. VCA calculations within the GWA

The DFT-LDA underestimates the band gaps of AlN, GaN, and InN which is a well-known shortcoming of the LDA for semiconductors. Thus, it is important to investigate the band-gap bowing also on the basis of a more reliable band-structure method. Therefore, at the next level of our calculations, we include quasiparticle corrections to the LDA band gaps within VCA. They are obtained from *GW* calculations based on the preceding LDA calculations. The dielectric screening is evaluated within the random-phase approximation (RPA). Details of the procedure can be found elsewhere.[10] The resulting band gaps for $Ga_xAl_{1-x}N$ are shown in Fig. 1, as well, and the respective bowing parameters are summarized in Table II. The bowing parameters for direct and indirect transitions between the QP bands are now slightly positive and the absolute value of the bowing has slightly decreased, as compared to that of the LDA gaps. The bowing parameters are given by $b_{dir}^{QP}=b_{ind}^{QP}=+0.05$ eV. Since the QP corrections to the indirect ($\Gamma\rightarrow X$) transitions are larger than those to the direct ($\Gamma\rightarrow\Gamma$) transitions, the direct–indirect transition now occurs at a smaller concentration $x_t^{QP}=0.37$ than in the LDA (see Table II). At x_t^{QP} we find a QP band gap of $E_g^{QP}(x_t^{QP})=4.9$ eV which is the largest direct band gap that can be realized in $Ga_xAl_{1-x}N$. The change of the band bowing due to the QP corrections (e.g., $b_{dir}^{LDA}=-0.15$ eV$\rightarrow b_{dir}^{QP}=+0.05$ eV) results from a slightly nonlinear dependence of the dielectric screening on the concentration. As an illustration, Fig. 2 shows the calculated macroscopic RPA dielectric constant for $Ga_xAl_{1-x}N$ as a function of x. It can be expressed as $\epsilon_\infty(x)=x\epsilon_\infty^{GaN}+(1-x)\epsilon_\infty^{AlN}+bx(1-x)$ with a bowing parameter of $b=-0.36$. For concentrations around $x=0.5$ the dielectric screening causes a nonlinear behavior of the QP correction to the gap. Weaker screening leads to stronger QP corrections; i.e., the QP corrections of the gap are stronger than linear in x with an additional upward bowing of 0.2 eV for the direct band gap. This also affects the concentration dependence of $b(x)$. For the direct band gap we find $b^{QP}(x)=(-0.25x+0.04)$ eV, resulting in $b^{QP}(x)=-0.19$ eV at high Ga concentrations ($x=0.9$). Although this value is remarkably lower in magnitude than the respective DFT-LDA result (cf. Table II), we find again the same qualitative behavior; i.e., b becomes less negative for decreasing x.

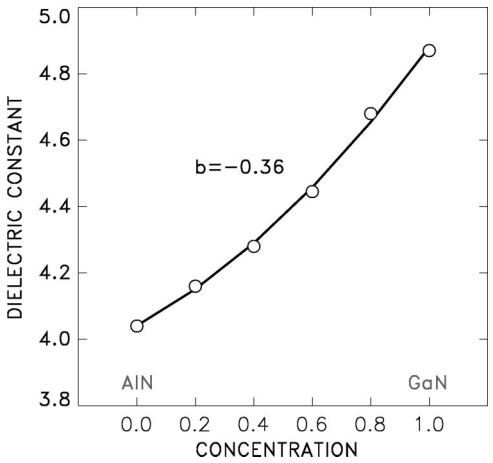

FIG. 2. Calculated dielectric constant of $Ga_xAl_{1-x}N$ as a function of concentration. The observed nonlinear behavior is the reason for the change in the VCA band-gap bowing when going from DFT-LDA to GWA calculations (cf. Fig. 1).

IV. RESULTS FOR $Ga_xIn_{1-x}N$

Before addressing the results of our calculations a brief survey on the experimental and theoretical literature seems useful.

A. Data from the literature

The metastable cubic phase can be synthesized by plasma-assisted molecular beam epitaxy (PA-MBE) on GaAs.[19] The band-gap bowing of zinc-blende $Ga_xIn_{1-x}N$ alloys has been analyzed recently.[19,20] The authors reported concentration dependent bowing of -1.4 eV (see Table III). The concentrations were derived from Rutherford backscattering experiments.

TABLE III. Experimental bowing parameters for the band gap of $Ga_xIn_{1-x}N$ in the restricted Ga-rich concentration regime, derived from optical spectroscopy.

Author	Structure	$b_{\text{Ga-rich}}$ [eV]
Goldhahn *et al.*[a]	zincblende	−1.4
Nakamura[b]	wurtzite	−1.0
Wetzel *et al.*[c]	wurtzite	−3.2
Takeuchi *et al.*[d]	wurtzite	−2.8
McCluskey *et al.*[e]	wurtzite	−2.9
Wetzel *et al.*[c]	wurtzite (ideal)	−3.8
McCluskey *et al.*[e]	wurtzite (ideal)	−4.2
Osamura *et al.*[f]	polymorph	−1.0

[a]Reference 19 and 20.
[b]Reference 44.
[c]Reference 45.
[d]Reference 46.
[e]Reference 47.
[f]Reference 48.

Hexagonal $Ga_xIn_{1-x}N$ can be grown on sapphire substrates by MOCVD.[44] Buffer layers of GaN or AlN are well suited to improve the crystalline quality of the epitaxial films.[44,45] Because $Ga_xIn_{1-x}N$ is characterized by a large miscibility gap from approximately $x=0.2$ to $x=0.8$, experimental investigations were only carried out for a few concentrations within the restricted regime from $x=0.8$ to $x=1.0$. Band-gap bowing of hexagonal $Ga_xIn_{1-x}N$ has been experimentally investigated by Nakamura,[44] Wetzel *et al.*,[45] Takeuchi *et al.*,[46] McCluskey *et al.*,[47] and Osamura *et al.*[48] For the results, see Table III. All these authors have found a concentration-dependent bowing function $b(x)$ and have pointed out that the lattice constant depends nonlinearly on concentration. Since the experimental determination of the concentration often relies on measuring the lattice constant and inverting Vegard's law, some earlier investigations[44] should be viewed with caution.

In order to discuss the concentration dependence of the direct band gap of $Ga_xIn_{1-x}N$ we will use two different types of bowing parameters. The *average* bowing parameter b corresponds to a quadratic fit of E_{gap} [analogous to Eq. (1)]. In addition, we consider a *restricted* bowing parameter $b_{\text{Ga-rich}}$ that describes the bowing in the Ga-rich range from $x=0.8$ to 1.0. We define $b_{\text{Ga-rich}}$ as the average of the concentration-dependent $b(x)$ between $x=0.8$ and $x=1.0$; i.e., $b_{\text{Ga-rich}}=b(0.9)$. This restricted bowing parameter thus corresponds to the experimental data obtained in the limited concentration range of $x=0.8$–1.0.

Various calculations have addressed the band-gap bowing in $Ga_xIn_{1-x}N$ (see the compilation in Table IV). A different bowing behavior of hexagonal and cubic $Ga_xIn_{1-x}N$ is supported by semiempirical VCA calculations by Pugh *et al.*[28] These authors calculated $b_{\text{Ga-rich}}=-2.08$ eV for cubic and $b_{\text{Ga-rich}}=-3.49$ eV for hexagonal $Ga_xIn_{1-x}N$. The latter result has been confirmed by an empirical VCA calculation[49] ($b_{\text{Ga-rich}}=-3.3$ eV). *Ab initio* VCA calculations[50] by Lambrecht[51] found a much lower *average* bowing for the cubic modification ($b_{LDA}=-0.60$ eV) and a concentration dependence of $b_{LDA}(x)=(0.32x-0.88)$ eV, which yields a restricted bowing of $b^{LDA}_{\text{Ga-rich}}=-0.59$ eV. Calculations employing the CEA (see Sec. V) have yielded slightly stronger *average* bowing parameters $b_{LDA}=-0.89$ eV (Ref. 51) and $b_{LDA}=-0.68$ eV (Ref. 13) with a concentration dependence of $b_{LDA}(x)=(1.05x-1.92)$ eV and $b_{LDA}(x)=(-0.10x-0.64)$ eV, respectively. For the concentration regime between 0.8 and 1.0 this leads to $b^{LDA}_{\text{Ga-rich}}=-0.98$ eV and $b^{LDA}_{\text{Ga-rich}}=-0.73$ eV, respectively. In a recent publication based on CEA calculations for 64-atom clusters, Ferhat and Bechstedt[14] have determined a larger bowing of −1.61 eV for $x=0.75$ which we have roughly extrapolated to a value of −1.65 eV at $x=0.9$, as given in Table IV. Note that $b_{LDA}(x)<0$ for all concentrations.

TABLE IV. Theoretical bowing parameters and their concentration dependences for the band gap of zinc-blende $Ga_xIn_{1-x}N$ extracted from band-gap results published in the literature.

Author	Method	$b(x)$ [eV]	$b_{\text{Ga-rich}}$ [eV]	b [eV]
Pugh *et al.*[a]	VCA	$-1.70x-0.55$	−2.08	−1.41
Lambrecht[b]	VCA	$+0.32x-0.88$	−0.59	−0.60
Lambrecht[b]	CEA	$+1.05x-1.92$	−0.98	−0.89
Teles *et al.*[c]	CEA	$-0.10x-0.64$	−0.73	−0.68
Ferhat *et al.*[d]	CEA		−1.65	

[a]Reference 28.
[b]Reference 51.
[c]Reference 13.
[d]Reference 14.

B. VCA calculations

The lattice constants of GaN (4.50 Å) and InN (4.98 Å) differ by more than 10%. It can thus be expected that significant internal relaxations will occur in $Ga_xIn_{1-x}N$, which cannot be handled by the VCA. The bowing parameters resulting from our VCA calculations are summarized in Table V. In fact, both within the LDA (first line) and in the GW QP theory (second line) we obtain bowing results in disagreement with experiment (cf. Table III). The bowing does not have a negative sign at all concentrations; nor does the restricted bowing parameter agree with the measured bowing at high concentration.

Another possible source of the discrepancy could be the neglect of the Ga $3d$ and In $4d$ semicore states which have been eliminated in constructing the 3+ pseudopotentials. Such states significantly affect the electronic properties of

TABLE V. VCA and CEA results for the band-gap bowing and its concentration dependence for zincblende $Ga_xIn_{1-x}N$. Different methods (LDA vs SIRC) and different pseudopotentials (PP's) have been used.

PP	Method	$b(x)$ [eV]	$b_{\text{Ga-rich}}$ [eV]	b [eV]
3+	VCA/LDA	$+1.65x-1.18$	+0.31	−0.36
3+	VCA/GW	$+1.90x-1.28$	+0.43	−0.36
13+	VCA/LDA	$-2.97x-0.99$	−3.66	−2.49
3+	CEA/LDA	$-0.08x-0.35$	−0.41	−0.50
13+	CEA/LDA	$+0.14x-0.87$	−0.74	−0.82
13+	CEA/SIRC	$+0.47x-1.09$	−0.71	−0.82

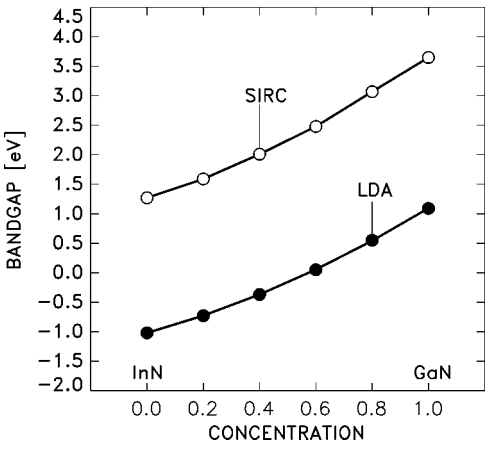

FIG. 3. Concentration-dependent band gap of $Ga_xIn_{1-x}N$ calculated within the CEA employing LDA and SIRC using 13+ pseudopotentials. Note that the SIRC corrections modify the absolute gap values but leave the bowing basically unchanged.

GaN and InN.[10,52,53] For a reliable description of the electronic structure they should be included in the calculation as valence states by using the corresponding 13+ pseudopotentials. The bowing parameters resulting from these calculations are shown in the third line of Table V. Apparently these results deviate even more strongly from the experimental data. The likely reason for this behavior is the completely different localization of the Ga 3*d* and In 4*d* states. Ga 3*d* states are nearly twice as strongly localized as In 4*d* states which makes it difficult to mix them in a meaningful way in terms of a virtual potential. The strong bowing can thus be identified as an artifact of the VCA when realized in terms of ionic pseudopotentials for very different atomic states.

The results discussed here show that the VCA is not a useful approximation for alloys of components with strongly differing lattice constants or when states with very different localization behavior are to be mixed. Instead, approaches like the cluster expansion approximation should be employed.

C. Cluster expansion results

The CEA maintains the individual character of the different atoms. It thus allows to incorporate the cationic *d* semicore states of Ga and In in a well-defined way and to investigate the role of internal structural relaxations, in particular of the different lengths of Ga-N and In-N bonds.

We first investigate the influence of the semicore *d* states keeping the geometry in the ideal zinc-blende structure with Vegard's law for the lattice constant. Again, we focus on the direct band gap and, in particular, on its bowing. The results are compiled in Table V and Fig. 3.

When the conventional 3+ pseudopotentials are employed in CEA calculations, the resulting band gaps (not shown in Fig. 3) are similar in magnitude to those of the VCA. Their bowing (fourth line in Table V), however, differs significantly from the corresponding VCA results, in particular in the high-concentration regime. The restricted bowing, e.g., changes from $+0.31$ eV to -0.41 eV, giving the correct sign (downward bowing) at all concentrations. Still, there are strong deviations from the experimental data.

Motivated by the importance of the cationic *d* states for the electronic structure of the pure materials GaN and InN, we now include the *d* states by using 13+ PP's. This has a significant effect on the magnitude of the LDA band gaps, which are now lower by more than 1 eV (see the lower curve of Fig. 3). Apart from this, the bowing of the band gap is also affected, resulting in the data given in the fifth line of Table V. The negative bowing is enhanced by 0.3 eV at all concentrations, yielding bowing parameters in good agreement with the CEA calculations by Lambrecht[51] ($b=-0.89$ eV) and Teles *et al.*[13] ($b=-0.68$ eV). In particular at high concentrations, our result of $b_{\text{Ga-rich}}=-0.74$ eV is in much better agreement with the experimental data than our VCA results. Nevertheless, there are still significant deviations from the measured data.

The significant underestimation of the LDA band gaps in the present 13+ PP calculations can be overcome by including QP corrections or, more easily, by incorporating SIRC corrections (see Sec. II). The resulting SIRC band gaps are indeed larger by more than 2 eV (see the upper curve in Fig. 3) and agree well with the measured data for GaN and InN. The bowing behavior, on the other hand, is only very weakly affected by the SIRC corrections (see Table V), yielding basically the same bowing parameters. We remind the reader that, on the basis of the discussion in Sec. III C, *GW* QP corrections can be expected to have only a minor influence on the bowing. This leads to the conclusion that the band-gap bowing is only weakly affected by electronic correlation effects and can be calculated accurately already within the LDA. If deviations from experiment remain, they can be expected to be caused by more intricate features of the geometric structure of the alloy which can not be accounted for by simply using a linear dependence of the lattice constant according to Vegard's law. These influences will be discussed in the next section.

D. Composition-dependent lattice constants and structural relaxations

The big advantage of the CEA is the possibility to study local structural relaxations and to carefully evaluate the lattice constant. Both issues have significant influence on the electronic properties of $Ga_xIn_{1-x}N$. Throughout this section we employ the LDA and use cationic 13+ PP's for Ga and In since 13+ PP's yield excellent structural properties for pure GaN and InN which are much more reliable than the results of 3+ PP's.

We discuss the influence of structural relaxations in four steps. The resulting band-gap parameters are compiled in Table VI. Figure 4, in addition, shows the band gap of $Ga_xIn_{1-x}N$ in the Ga-rich regime—i.e., for Ga concentrations between 0.8 and 1.0. The figure reveals that the band gaps resulting from the four different approximations are basically linear functions of x in this restricted concentration regime. The band-gap variation with x as resulting from Vegard's law (no bowing) is included for comparison as the dashed line. To allow for a direct comparison with experi-

TABLE VI. CEA band-gap bowing parameters and their concentration dependence for $Ga_xIn_{1-x}N$ as calculated for different sets of lattice constants. "Vegard experiment" stands for linear interpolated experimental lattice constants (see fifth line of Table V. In "Vegard theory" the theoretical lattice constants for GaN and InN have been connected linearly, while "Theory" shows bowing parameters calculated for the ideal zinc-blende configuration and for structurally relaxed clusters in the unit cell. All our CEA calculations have been carried out with 13+ semicore pseudopotentials.

	Lattice constant	Structure	$b(x)$ [eV]	$b_{\text{Ga-rich}}$ [eV]	b [eV]	$E_{gap}^{x=0.82}$ [eV]
[1]	Vegard experiment	ideal	$+0.14x-0.87$	-0.74	-0.82	2.84
[2]	Vegard theory	ideal	$+0.06x-0.99$	-0.94	-0.96	2.81
[3]	Theory	ideal	$-1.32x-1.08$	-2.23	-1.74	2.65
[4]	Theory	relaxed	$-0.96x-0.80$	-1.66	-1.28	2.73
	Experiment [a]			-1.4		2.75

[a]References 19 and 20.

ment, we rescale the calculated $E_{gap}(x)$ curves linearly to match the experimental band gaps of $E_{gap}^{InN}(0)=1.9$ eV and $E_{gap}^{GaN}(1)=3.2$ eV. We compare our results with the data measured by Goldhahn *et al.*, in particular with the gap energy of 2.75 eV at $x=0.82$.[19,20]

The first set of data is the same as discussed in the preceding sections: i.e., the results for the ideal zinc-blende structure with the lattice constant depending linearly on concentration (cf. fifth line of Table V). As discussed above, this leads to a bowing which is too weak, in particular for large $x(b_{\text{Ga-rich}}=-0.74$ eV). After rescaling we obtain a value of $E_{gap}(0.82)=2.84$ eV, which is larger than the measured value of $E_{gap}^{exp}(0.82)=2.75$ eV.[19,20]

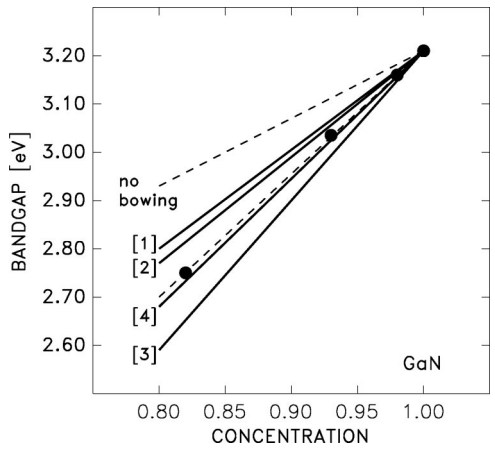

FIG. 4. Band gap of $Ga_xIn_{1-x}N$ in the Ga-rich regime. The lines [1]–[4] have been obtained from CEA calculations using DFT-LDA and 13+ PP's. For curves [1] and [2] the lattice constant is assumed to interpolate linearly (Vegard's law) between the experimental or theoretical lattice constants of InN and GaN, respectively. Curves [3] and [4] have been obtained for total-energy-optimized lattice constants neglecting [3] or including [4] internal relaxation, respectively. In all cases the band-gap data have been rescaled to match the experimental band gap for pure InN $[E_{gap}^{InN}(0)=1.9$ eV] and GaN $[E_{gap}^{GaN}(1)=3.2$ eV] (Refs. 19 and 20). The dots denote experimental results by Goldhahn *et al.* (Refs. 19 and 20) connected by a dashed line to guide the eye. The upper dashed line denotes the linear Vegard-like interpolation between the experimental band gaps of InN and GaN (i.e., with zero bowing).

For the second set of data, we check the lattice constant of the pure materials GaN and InN. From our 13+ PP's we obtain a theoretical lattice constant of 4.45 Å for GaN which is slightly lower than the experimental value of 4.50 Å and 4.98 Å for InN in coincidence with the experimental value of 4.98 Å. These may seem to be minor deviations. One has to keep in mind, however, that the band structure is quite sensitive to the lattice constant. When we assume that the lattice constant of the alloy interpolates linearly between these *theoretical* lattice constants of GaN and InN rather than between the experimental ones, the band-gap bowing changes to $b_{\text{Ga-rich}}=-0.94$ eV and the band gap drops to $E_{gap}(0.82)=2.81$ eV. This change originates from the fact that the theoretical lattice constant resulting from total energy optimization agrees with experiment for InN while it deviates slightly from the experimental value for GaN.

In the third step, we go beyond Vegard's assumption and optimize the lattice constant at each concentration x. At each lattice constant a, we statistically average the total energy of the clusters, yielding a total energy $E_{tot}(a,x)$ for a given concentration x. The optimization with respect to a now gives a theoretical lattice constant $a(x)$ for a given concentration. These lattice constants are displayed in Fig. 5(a) (open circles). In fact, they exhibit a significant deviation from the linear interpolation (i.e., from Vegard's law, shown by the dashed line). At intermediate concentrations ($x\sim0.5$) the optimized lattice constant is about 0.05 Å larger than the linearly interpolated one. We believe that this behavior is not related to the different elastic constants of GaN and InN. In fact, we obtain bulk moduli of 2.4 Mbar for GaN and 1.8 Mbar for InN. These data would suggest that, since the Ga-N bonds are stiffer than the In-N bonds, the lattice constant of the alloy should be even smaller than resulting from the linear interpolation. The expansion of the alloy is rather related to the nonparabolicity (or anharmonicity) of the bond-length dependence of the bond energies—i.e., to the fact that at large amplitudes bonds are easier expanded than compressed. To make this point more quantitative we consider the individual Ga-N and In-N bonds. When GaN is expanded to the lattice constant of InN (i.e., stretching all Ga-N bonds by 0.22 Å), the energy associated with a Ga-N

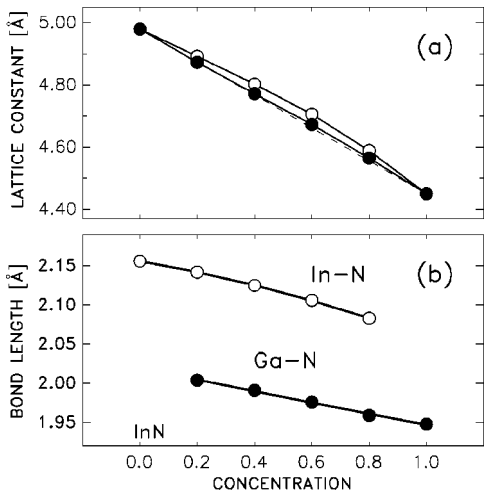

FIG. 5. (a) Concentration-dependent lattice constant of $Ga_xIn_{1-x}N$ calculated within the CEA employing DFT-LDA and 13+ pseudopotentials. The dashed line denotes the linear interpolation between the theoretical lattice constants of InN and GaN (Vegard's law). The open circles have been obtained from zinc-blende-structured clusters, while the solid circles include the internal relaxation effects as shown in (b) (see text). (b) Calculated Ga-N and In-N bond lengths obtained from internal structural optimization.

bond does not increase by 0.44 eV (as suggested by the GaN bulk modulus) but by 0.35 eV, only. On the other hand, when InN is compressed to the lattice constant of GaN the In-N bond energy increases by 0.54 eV, which is much higher than the value of 0.39 eV corresponding to the InN bulk modulus. Since we are still considering the ideal zinc-blende crystal for the alloy, all bond lengths (Ga-N and In-N) scale proportional to the lattice constants which means that (at intermediate concentrations) both bond lengths will deviate significantly from their equilibrium values. The fact that, at such large amplitude, it is easier to expand the Ga-N bonds rather than to compress the In-N bonds finally results in effective lattice constants larger than the linear average. The enlarged lattice constants lead to smaller gaps at intermediate concentration (note that $\partial E_{gap}/\partial a = -3.1$ eV/Å for GaN and -2.0 eV/Å for InN), resulting in an enhanced bowing of $b(x) = (-1.32x - 1.08)$ eV. At $x = 0.82$, the rescaled gap energy amounts to 2.65 eV, which is now considerably lower than the experimental value of 2.75 eV (see Fig. 4).

As the fourth step of our investigation, we allow for full internal relaxation of the clusters in order to overcome the significant strain which is induced in both the In-N and the Ga-N bonds when the calculations are restricted to the ideal zinc-blende structure, as discussed above. In fact, we observe a significant relaxation of both types of bonds towards their intrinsic equilibrium bond length (1.95 Å for Ga-N and 2.16 Å for In-N) accompanied by a large gain in total energy. Again, we evaluate the total energy as a function of the lattice constant and the concentration x, yielding a concentration-dependent lattice constant. These lattice constants [shown by the solid circles in Fig. 5(a)] are much lower than the ones obtained without relaxation. In fact, they are now again quite close to the linear interpolation of the lattice constants, confirming that Vegard's law is a rather good approximation for the lattice constants even in $Ga_xIn_{1-x}N$.

Figure 5(b) shows the average Ga-N and In-N bond lengths as a function of concentration. Apparently, they are fairly close to their equilibrium values with only slight modifications due to the alloy environment. The In-N bonds become slightly shortened at increasing Ga concentrations but this shortening is one order of magnitude smaller than the shortening of the lattice constant. The Ga-N bonds become slightly longer with increasing In concentration which is again one order of magnitude smaller than the increase of the lattice constant when going from GaN to InN.

The relaxation of the bonds and the corresponding reduction of the lattice constant enhances the band-gap energy accompanied by a weakening of the bowing to $b(x) = (-0.96x - 0.80)$ eV. In particular at high Ga concentrations, the band gaps change significantly. At $x = 0.82$, we now obtain a gap energy of $E_{gap}(0.82) = 2.73$ eV in good agreement with the experimental value of 2.75 eV.[19,20] This final result yields the best agreement of the calculated bowing parameter $b_{\text{Ga-rich}} = -1.66$ eV with the experimental result of -1.4 eV from Refs. 19 and 20. Furthermore, it yields the theoretically best-founded concentration-dependent band gap in the Ga-rich regime (which is labeled as approximation [4] in Fig. 4).

V. CONCLUSION

In conclusion, we have investigated the electronic structure of two wide-band-gap III-nitride alloys $Ga_xAl_{1-x}N$ and $Ga_xIn_{1-x}N$, within *ab initio* density functional and quasiparticle theory. We have focused in particular on the nonlinear concentration dependence of the band gap expressed in terms of its bowing parameter b or bowing function $b(x)$, respectively. Both the virtual crystal and cluster expansion approximation have been employed to simulate the alloy statistically. Based on density functional theory we have evaluated *GW* quasiparticle corrections, as well as self-interaction and relaxation corrections, to overcome the systematical underestimation of the band gap in semiconductors within the LDA.

For $Ga_xAl_{1-x}N$, in which the lattice mismatch between AlN and GaN amounts only to some 3%, our VCA calculations yield a reasonable description of the alloy. The band gap depends nearly linearly on the alloy concentration x both within the LDA and within the GWA. This is in agreement with most experimental data.

In the case of $Ga_xIn_{1-x}N$, the situation is more complicated due to the large lattice mismatch between GaN and InN amounting to some 10% and due to the influence of the Ga $3d$ and In $4d$ semicore states. A reliable description is achieved within the CEA including the d electrons among the valence states. A careful investigation of the internal lattice structure shows that significant bond-length relaxation takes place which strongly influences the electronic band gap. The fully relaxed structure yields electronic-structure results that

are in good agreement with experimental data. This indicates that a reliable investigation of such alloys requires to treat both the electronic and geometric structure on equal footing.

In all cases we find that electronic many-body effects, as evaluated within the GWA or SIRC-DFT, significantly affect the absolute size of the band gaps but leave the bowing nearly unaffected.

ACKNOWLEDGMENTS

The authors acknowledge financial support by the Deutsche Forschungsgemeinschaft (Bonn,Germany) under Grant Nos. Ro-1318/2-1 and Po-215/15-1. Computational resources have been provided by the Bundeshöchstleistungsrechenzentrum Stuttgart (HLRS).

[1] W.R.L. Lambrecht and B. Segall, in *Properties of the III-Nitrides*, edited by J.H. Edgar (EMIS, London, 1994).

[2] L. Nordheim, Ann. Phys. (Leipzig) **9**, 607 (1931).

[3] J.S. Faulkner, in *Modern Theory of Alloys*, edited by J.W. Christian, P. Haase, and T.B. Massalski [Prog. Mater. Sci. **27**, 3 (1982)].

[4] R. Kikuchi, Phys. Rev. **81**, 988 (1951).

[5] J.M. Sanchez and D. de Fontaine, Phys. Rev. B **17**, 2926 (1978).

[6] J.M. Sanchez, F. Ducastelle, and D. Gratias, Physica A **128**, 334 (1984).

[7] D. Vogel, P. Krüger, and J. Pollmann, Phys. Rev. B **55**, 12 836 (1997).

[8] C. Stampfl, C.G. Van de Walle, D. Vogel, P. Krüger, and J. Pollmann, Phys. Rev. B **61**, R7846 (2000).

[9] M.S. Hybertsen and S.G. Louie, Phys. Rev. B **34**, 5390 (1986) and references therein.

[10] M. Rohlfing, P. Krüger, and J. Pollmann, Phys. Rev. B **57**, 6485 (1998).

[11] J.W.D. Connolly and A.R. Williams, Phys. Rev. B **27**, 5169 (1983).

[12] S.H. Wei, L.G. Ferreira, J.E. Bernard, and A. Zunger, Phys. Rev. B **42**, 9622 (1990).

[13] L.K. Teles, J. Furthmüller, L.M.R. Scolfaro, J.R. Leite, and F. Bechstedt, Phys. Rev. B **62**, 2475 (2000); **63**, 085204 (2001). Note that for a direct comparison of our results with the results of these and the following reference b has to be interchanged with $-b$ and x with $1-x$.

[14] M. Ferhat and F. Bechstedt, Phys. Rev. B **65**, 075213 (2002).

[15] D. Schwabe and W. Mader (unpublished).

[16] D. Gerthsen, B. Neubauer, C. Dieker, R. Lantier, A. Rizzi, and H. Lüth, J. Cryst. Growth **200**, 353 (1999).

[17] A. Rubio, J.L. Corkill, M.L. Cohen, E.L. Shirley, and S.G. Louie, Phys. Rev. B **48**, 11 810 (1993).

[18] T. Lei, T.D. Moustakas, R.J. Graham, Y. He, and S.J. Berkowitz, J. Appl. Phys. **71**, 4933 (1992).

[19] R. Goldhahn, J. Scheiner, S. Shokhovets, T. Frey, U. Köhler, D.J. As, and K. Lischka, Phys. Status Solidi B **216**, 265 (1999).

[20] R. Goldhahn, J. Scheiner, S. Shokhovets, T. Frey, U. Köhler, D.J. As, and K. Lischka, Appl. Phys. Lett. **76**, 291 (2000).

[21] T.L. Tansley and C.P. Foley, J. Appl. Phys. **59**, 3241 (1986).

[22] M. Buongiorno-Nardelli, K. Rapcewicz, E.L. Briggs, C. Bungaro, and J. Bernholc, in *III-Nitrides*, edited by F.A. Ponce, T.D. Moustakas, I. Akasaki, and B.A. Monemar, Mater. Res. Soc. Symp. Proc. 449 (Materials Research Society, Pittsburgh, 1997), p. 893.

[23] W. L. Lambrecht, in *Semiconductors and Semimetals*, edited by E. Weber and B. Willardson (Academic Press, New York, 1996).

[24] We use the decay constants {0.2,0.6,1.8} for Al, Ga, and In. For N the decay constants {0.4,1.6,6.4} are employed. When semicore d states are explicitly included as valence states the original set of decay constants for Ga and In is extended to {0.18,0.55,1.60,5.70,17.1}. All decay constants are given in atomic units.

[25] D.R. Hamann, M. Schlüter, and C. Chiang, Phys. Rev. Lett. **43**, 1494 (1979); D.R. Hamann, Phys. Rev. B **40**, 2980 (1989).

[26] G. Bachelet, D.R. Hamann, and M. Schlüter, Phys. Rev. B **26**, 4199 (1982).

[27] W.J. Fan, M.F. Li, T.C. Chong, and J.B. Xia, J. Appl. Phys. **79**, 188 (1996).

[28] S.K. Pugh, D.J. Dugdale, S. Brand, and R.A. Abram, J. Appl. Phys. **86**, 3768 (1999).

[29] L. Bellaiche and D. Vanderbilt, Phys. Rev. B **61**, 7877 (2000).

[30] L. Kleinman and D.M. Bylander, Phys. Rev. Lett. **48**, 1425 (1982).

[31] L. Vegard, Z. Phys. **5**, 17 (1921).

[32] J. Hagen, R.D. Metcalfe, D.K. Wickenden, and W. Clark, J. Phys. C **11**, L143 (1978).

[33] Y. Koide, H. Itoh, N. Sawaki, J. Akasaki, and M. Hashimoto, J. Electrochem. Soc. **133**, 1956 (1986).

[34] E.A. Albanesi, W.R.L. Lambrecht, and B. Segall, Phys. Rev. B **48**, 17 841 (1993).

[35] Bal K. Agrawal, S. Agrawal, P.S. Yadav, and S. Kumar, J. Phys. C **9**, 1763 (1997).

[36] A.F. Wright and J.S. Nelson, Appl. Phys. Lett. **66**, 3051 (1995).

[37] J. Fritsch, O.F. Sankey, K.E. Schmidt, and J.B. Page, J. Phys. C **11**, 2351 (1999).

[38] S. Yoshida, S. Misawa, and S. Gonda, J. Appl. Phys. **53**, 6844 (1982).

[39] Y. Koide, H. Itoh, R.H. Khan, K. Hiramatu, N. Sawaki, and J. Akasaki, J. Appl. Phys. **61**, 4540 (1987).

[40] K. Itoh, H. Amano, K. Hiramatsu, and T. Akasaki, Jpn. J. Appl. Phys., Part 1 **30**, 1604 (1991).

[41] M.R.H. Khan, Y. Koide, H. Itoh, N. Sawaki, and I. Akasaki, Solid State Commun. **60**, 509 (1986).

[42] M.A. Khan, R.A. Skogman, R.G. Schulze, and M. Gershenzon, Appl. Phys. Lett. **43**, 492 (1983).

[43] D.K. Wickenden, C.B. Bargeron, W.A. Bryden, J. Miragliotta, and T.J. Kistenmacher, Appl. Phys. Lett. **65**, 2024 (1994).

[44] S. Nakamura, J. Vac. Sci. Technol. A **13**, 705 (1995).

[45] C. Wetzel, T. Takeuchi, S. Yamaguchi, H. Katoh, H. Amano, and I. Akasaki, Appl. Phys. Lett. **73**, 1994 (1998).

[46] T. Takeuchi, H. Takeuchi, S. Sota, H. Sakai, H. Amano, and I. Akasaki, Jpn. J. Appl. Phys., Part 2 **36**, L177 (1997).

[47] M.D. McCluskey, C.G. van de Walle, C.P. Master, L.T. Romano, and N.M. Johnson, Appl. Phys. Lett. **72**, 2725 (1998).

[48] K. Osamura, K. Nakajima, and Y. Muramaki, Solid State Commun. **11**, 617 (1972).
[49] B.C. Lee, J. Korean Phys. Soc. **35**, 8 (1997).
[50] Note that the calculations by Lambrecht (Ref. 51) are not strictly VCA like. Since the author used a linear average of (energy dependent) LMTO parameters, the method is more closely related to the *average T-matrix* approximation.
[51] W.R.L. Lambrecht (unpublished).
[52] F. Aryasetiawan and O. Gunnarsson, Phys. Rev. B **54**, 17 564 (1996).
[53] V. Fiorentini, M. Methfessel, and M. Scheffler, Phys. Rev. B **47**, 13 353 (1993).